Available online at www.sciencedirect.com
SCIENCE DIRECT®
Physica C 423 (2005) 37–44
PHYSICA C
www.elsevier.com/locate/physc

Design, construction and performance of an EMS-based HTS maglev vehicle

Chen Gu [a,*], Menglin Liu [a], Huawei Xing [b], Tong Zhou [b], Wensheng Yin [c], Jun Zong [d], Zhenghe Han [a]

[a] *Applied Superconductivity Research Center, Department of Physics, Building LiZhai, Room 102, Tsinghua University, Beijing 100084, China*
[b] *Department of Automation, Tsinghua University, Beijing 100084, China*
[c] *Department of Precision Instruments and Mechanology, Tsinghua University, Beijing 100084, China*
[d] *Innova Superconductor Technology Co., Ltd., Beijing 100176, China*

Received 14 October 2004; received in revised form 24 February 2005; accepted 28 March 2005

Abstract

A laboratory-scale EMS-based HTS maglev vehicle operating over a 1.5 m guideway has been successfully constructed. The fully integrated system consists of a vehicle chassis, four dependent magnetic circuits, four distance sensors, and control and power amplification circuits. As key component of the system, each magnetic circuit includes a U-shape iron core with one HTS coil forming each pole. Eight HTS coils made of Bi-2223 multi-filamentary tape were used to provide the magnetic motive force. Several questions relating to the unique characteristics of the HTS material in a controlled magnetic circuit are discussed. The most important consideration for such applications is that the anisotropic critical current of the Bi-2223/Ag tape depends strongly on the magnetic field. The commercially available FEA software ANSYS was used to simulate the field distribution along the magnetic circuit and HTS coil winding, and thereby identify how the magnetic circuit alters the field distribution in the coil winding and therefore also the critical current. A general optimization process is described for finding the best position in the U-shape iron core to hold the HTS coils. In this process the critical current of the HTS tape and the force–current characteristic of the magnetic circuit are considered synthetically. The results demonstrate the feasibility and stability of HTS material in a typical maglev system and other similar controllability applications.

PACS: 84.71.Ba

Keywords: Bi-2223/Ag; HTS; Maglev; Vehicle

* Corresponding author. Tel.: +86 10 62785770; fax: +86 10 62785913.
E-mail address: guchen@mail.tsinghua.edu.cn (C. Gu).

0921-4534/$ - see front matter © 2005 Elsevier B.V. All rights reserved.
doi:10.1016/j.physc.2005.03.021

1. Introduction

The availability of the high critical current Bi-2223/Ag multi-filamentary tape makes it a good candidate as a substitute for conventional material in the coil used in typical EMS-based maglev systems. The main requirement for the coil in such applications is the ability to implement an active controlled current variation at frequencies up to 10 Hz to ensure stable suspension. This requirement limits the application of LTS coils in dynamic applications, where thermal dissipation generated by hysteresis losses would make LTS coils unstable. This problem was partially solved by hybrid-coil structure developed by Grumman Co. Ltd. in 1995 [1] where the LTS coil runs at a DC state with a current variation less than 1 Hz providing most of lift force, and with two additional normal copper-based coils for carrying active control signal out to 10 Hz were equipped simultaneously. Although the unwanted hysteresis losses were overcome by this structure, the cost in cryogenic requirement, and the system complexity forced these authors to consider the use of HTS material in a subsequent publication [2]. The most recent design attempt of a HTS maglev suspension demonstrator was done by collaborations between several UK groups as [3–6].

In this paper, the design, construction, and subsequent testing of a new maglev vehicle by using HTS coils are reported. We focus mainly on two points. First, the system and the status of development are briefly introduced, including information concerning the magnetic circuit, the HTS coils and the cryostat design and fabrication. Secondly, the effect on the magnetic circuit design arising from the field dependence of the critical current in HTS tape is discussed. To achieve this goal the commercially available Finite Element Analysis (FEA) package ANSYS is used to simulate the field distribution along the magnetic circuit and coil winding. The simulated results are compared with the $I(B)$ curve derived from short sample measurements, which are always regarded as a design basis for HTS coil. The first requirement for a HTS coil design is to guarantee that the operating current is below the critical current of the Bi-2223/Ag tape. This design idea was systematically studied and widely accepted for the general HTS coil fabrication [7,8]. In this study, we put it into application of controlled magnetic circuit and further present an experimental attempt at a design solution, which illustrates a method for finding the the optimum location for housing two HTS coils in the U-shape iron core where the critical current of Bi-2223 tape, current–force curves of the magnetic circuit as well as the choice of controller design are considered synthetically. The design is specific to the situation where two HTS coils are placed in parallel onto two poles of the U-shape iron core.

2. System design and construction

2.1. Basic information of the vehicle

In collaboration with three departments of Tsinghua university, a small 46 kg experimental vehicle operating along a 1.5 m guideway was successfully constructed in May, 2004. Configurations of the vehicle and the guideway are shown in Fig. 1. The vehicle chassis as well as four magnetic circuits weight around 40 kg and the system is designed to give an overall lift force of 80 kg with a nominal operating air gap of 5 mm. The vehicle includes four main components: a chassis as the vehicle skeleton, four magnetic circuits installed at each corner of the chassis to provide the lift

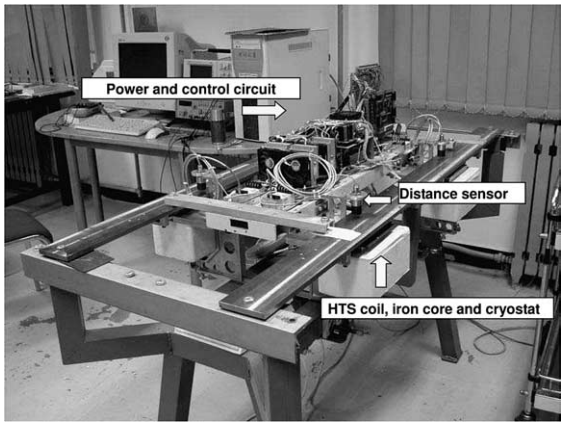

Fig. 1. Configuration of the EMS-based maglev vehicle.

Table 1
Specifications of the Bi-2223/Ag multi-filamentary tape

Parameter	Unit	Value
Dimension of the tape	mm × mm	4.1 × 0.23
Number of filaments		61
Critical current	A	41.2
N-value		12.3
Minimum bending diameter	mm	⩾50
Filling factor	%	32.4

force, a position sensor capable of measuring the variation of the air gap, and electronic control and amplification circuits. To achieve the levitation, the HTS coils were primarily operated at an equilibrium current 3.8 A, which is able to generate a vertical attraction force to balance the self-weight (46 kg) at an equilibrium location (5 mm). At the same time small alternate current run in the same coils, thus providing the regulating force to maintain the air gap around the equilibrium location.

A 600 m long Bi-2223/Ag multi-filamentary tape provided by Innova Superconductor Technology Co. Ltd. was used for the HTS coils. The specifications of the tape, derived from short sample measurement, are listed in Table 1. This tape was coated with epoxy paint of thickness about 10 μm to provide a turn-to-turn insulation.

A switch mode current power supply with four dependent amplification circuits was used. The power dissipation for each circuit under steady current 3.8 A is 20 W, yielding a total power dissipation of the system 80 W.

A classical lead-lag compensator was found to be very effective in achieving the controllability requirements, even when the load was varied to almost 84% of its original value. Details of this component will be published separately.

2.2. Magnetic circuit design and construction

Prior to the vehicle application, the property of the HTS magnetic circuit is studied in a mechanical lever as shown in Fig. 2. The magnetic circuit consists of a U-shape iron core, two HTS coils wrapped around each pole, and a cubic cryostat with two cylinders inside to separate the iron core

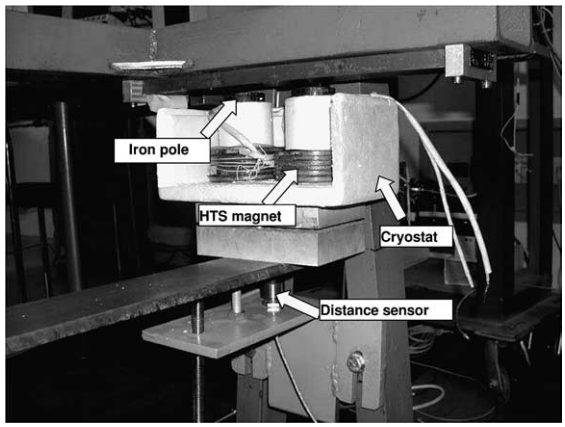

Fig. 2. Configuration of the magnetic circuit.

from the liquid nitrogen. The main parameters of the magnetic circuit is listed in Table 2.

The U-shape iron core has a quasi-uniform circular cross-section with diameter 45 mm. The core was constructed from laminated silicon steel with thickness 0.23 mm. The same material was also used to construct the rail mounted at a fixed point below the guideway.

Each HTS coil consists of three double-wound pancakes stacked coaxially without a bobbin. The absence of the bobbin in this design shortens the distance between the iron core and HTS coils, and hereby reduces the flux leakage as much as possible. Each pancake uses approximately 25 m of tape, yielding a total tape consumption of 75 m for each coil. The connection between the pancakes uses an ordinary Sn40–Pb60 solder, whose electrical resistance is the composite of the Ag alloy and Sn–Pb solder. Using a 3 cm overlapped area, the joint resistance could be contained within 50 nΩ, as accurately measured by a field decay method [9]. The final coils was impregnated with epoxy resin

Table 2
Main parameters of the magnetic circuit

Parameter	Unit	Value
U-core diameter	mm	45
Distance between tow poles	mm	46
Pole height	mm	120
Airgap between poles and rail	mm	5
Total weight	kg	7.2

Table 3
Main parameters of the HTS coil

Parameter	Unit	Value
Inner diameter	mm	60.0
Outer diameter	mm	80.0
Height	mm	31.4
Turns		270
Critical current	A	13.57
Magnetic constant	T/A	0.0054
Inductance	mH	231.8

Note that the self-inductance is conducted on the magnetic circuit with air gap 5 mm. This value is determined by taking the two coils as a whole.

to form an integral structure. The main parameters of the coil are summarized in Table 3 . No elaborate quench protection system was included because even for operation at the critical current 13.57 A the energy stored in the coils is small (21.3 J).

The cryostat was designed primarily to be a non-eddy current structure. To achieve this goal, all components of the cryostat were made from non-conductive material. A plastic foam injection moulding technique was applied to the cryostat fabrication, resulting in an integral, non-eddy current, light-weight cryostat, shown in Fig. 2. The thickness of wall adjacent to the pole of the iron core is little smaller than the other parts of container. The purpose of this design is, as for the the non-bobbin structure of the HTS coils, to decrease the flux leakage as much as possible. The cryostat can contain 1.1 l nitrogen; this amount is sufficient to keep the HTS coil in a superconducting state for at least 1.5 h.

3. HTS coil design and magnetic circuit optimization

One of the most important factors to take account of in a HTS coil design is the fact that the anisotropic critical current of the a HTS tape is very sensitive to the magnetic field, especially when the field is perpendicular to the tape wide surface, see Fig. 3. It is also known that the use of the high permeability ferromagnetic iron core can greatly alter the flux distribution within the coil winding, leading to an increase or decrease in the critical current. Voltage–current measurement has been

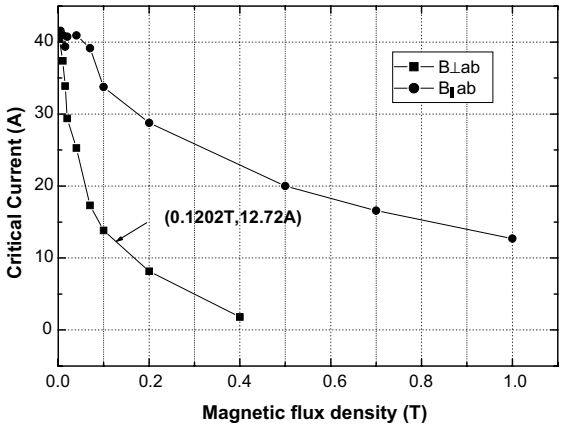

Fig. 3. Critical current as determined from short sample measurement as a function of applied field.

carried out for the coil with and without a U-shape iron core, respectively. The results, shown in Fig. 4, show an obvious difference between the two configurations. In contrast to the general expectation that the iron core would guide the flux and as a consequence, increase the critical current, the critical current with a U-shape iron core is about 2.1 A smaller than the no-core case. Using the commercially available FEA software package ANSYS, the simulated flux density along the radial direction of the empty coil for an exciting current of 13.57 A was calculated; the results are plotted in Fig. 5. The same calculation was performed for the whole magnetic circuit using a 3D

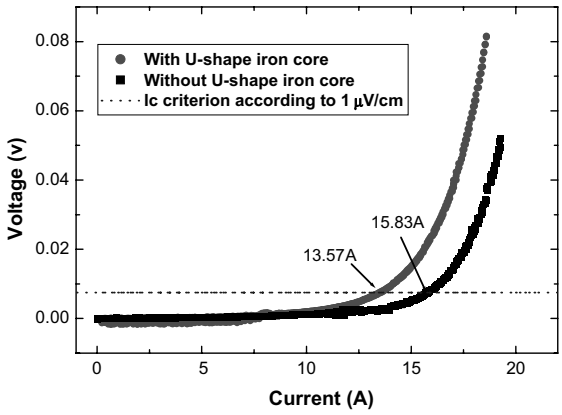

Fig. 4. Comparison of the voltage–current characteristics of the HTS coil with or without U-shape iron core.

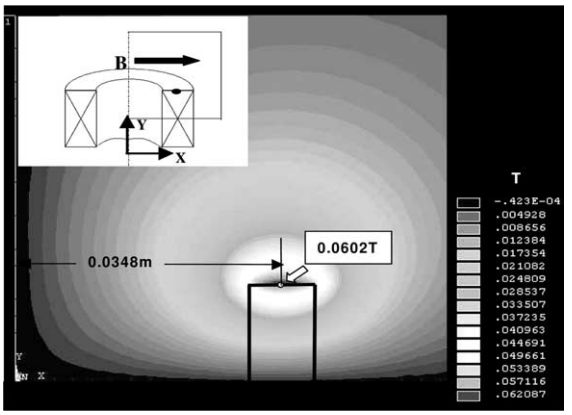

Fig. 5. Radial field distribution in the empty coil excited with current = 13.57 A. As a result of symmetry, only one quarter of the total area is modelled. The gray gradient in this figure represents the amplitude of the radial field.

mode. The results are shown in Fig. 6. Note that here the position of the coils was close to the bottom of the cryostat, as shown in Fig. 2 (i.e. not far away from the bottom of the two poles). The difference in characteristics for coils with or without an iron core can be understood from inspection of the FEA calculations in conjunction with the $I(B_{\perp})$ curve (Fig. 3). The maximum radial field for the no-core coil occurs in the middle turns of the outmost pancakes, with a value of 0.0604 T. However, the peak radial field in the winding with a U-shape iron core is only found at the side between the two poles reaching a much higher value of 0.1202 T. The difference arises because the flux leakage between the two poles makes a significant contribution to the radial component of the field, which, as it well known, is the most important field component for governing the behavior of the critical current. From this point of view, the HTS coil should be placed at the back leg of the U-shape core as previously reported [3]. As shown in Figs. 4 and 5, we also found that the measured I_c of 13.57 A is slightly higher than the value predicted by short sample measurements. This is because the peak field is found only within a relatively small region between the two poles. Other parts along this turn do not experience such high field, and therefore the critical current measured by a short sample will be smaller than the data given for measurement of the coil as a whole. For operation at measured critical current of 13.57 A, the critical current is exceeded at some local points, in particular the points between the two poles. For a practical implementation, care should therefore be taken of the current in this region.

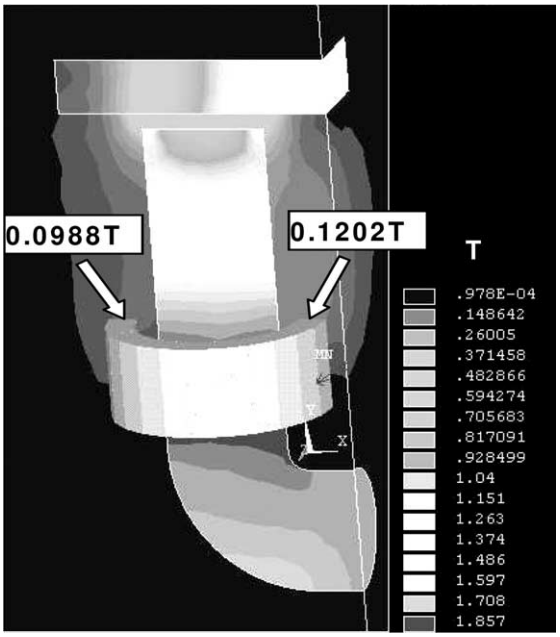

Fig. 6. Flux distribution in a coil with U-shape iron core. As a result of symmetry, only one quarter of the area is modelled. Here the value marked in the figure corresponds to value in the direction parallel to the X-axis. A symmetrical point is also selected for comparison.

As described earlier, the coils were located in parallel at the bottom of the cryostat. In fact, for a given winding geometry of the HTS coils, the location of the coils in the iron core is of critical importance to the system performance, and gives rise to two major problems. The first is concerned with the critical current of the Bi-2223/Ag tape. The second problem is associated with the nonlinear force–current characteristics and saturation of the iron core. The system performance is mostly determined by the combination of these two factors as a whole. For the purposes of investigating these problems, four reference points labelled A, B, C and D have been selected along the poles of the iron core. At each position (see Fig. 7) the measurement of HTS coil voltage–current characteristics and the magnetic circuit force–current curve

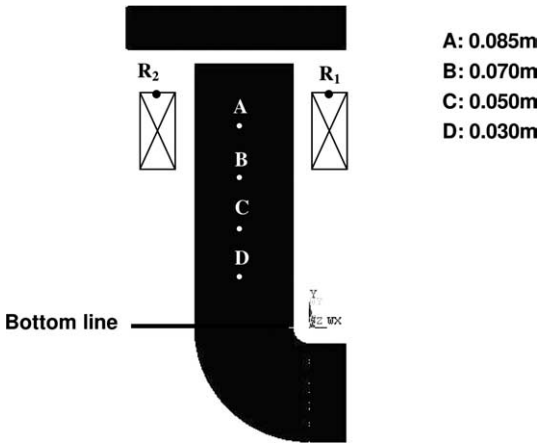

Fig. 7. Cross-section of the U-shape iron core showing the locations A, B, C and D, at different distances from the bottom line. Location D is used in the practical implementation. R1 and R2 are two reference points for field comparison.

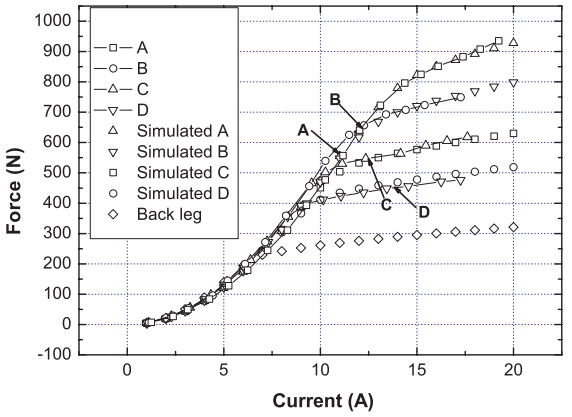

Fig. 9. Comparison of the force–current characteristics of the magnetic circuit for coils located at different points. The forces from A to D are 555, 641, 545 and 445 N, respectively. The simulation results for each case, as well as for the case of the coil placed at the back leg of iron core, are also shown.

have been carried out, respectively, as shown in Figs. 8 and 9. Results obtained from the voltage–current curves show that the critical current of the Bi-2223/Ag tape decreases as the distance between coils and the end of the poles is shortened. This can be partially explained by the fact that apart from the flux leakage between the two poles, the fringe effect at the end of the pole also contributes greatly to the radial component of the field. The closer the coils approach to the end of the pole, the more intensive should be the fringe effect and thus the smaller the critical current. However,

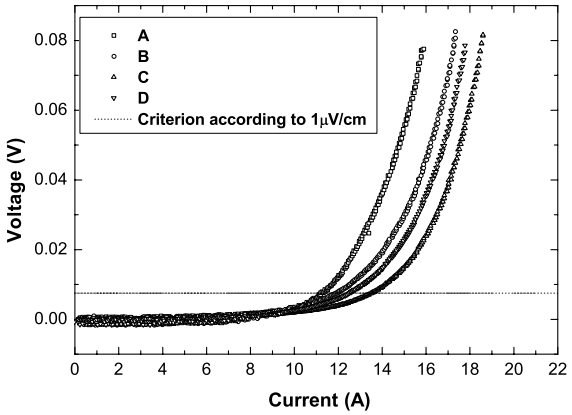

Fig. 8. Comparison of the voltage–current characteristics of the coil for different locations.

the force–current performance functioned inversely with such a distance variation. The curves in Fig. 9 show that the initial force–current curves are almost identical to each other, while an obvious improvement for position A and B was observed in the high current region. To further understanding these curves, simulated field distributions for each case were calculated and are given in Fig. 10. As can be seen in Fig. 10, the radial field in the reference points 1 and 2 increases as the coils are moved closer to the pole ends, which is in agreement with the voltage–current measurements. It is also evident that as the coils was moved towards the end of the pole, the maximum flux flowing through the middle part of the U-shape iron core is greatly released and which in turn will shift the saturation point to the high current region and therefore leads to observed improved force–current characteristics. Consequently the choice of coil location is a compromise between the force–current curve and voltage–current curve, as well as the saturation property of the iron core. For example, the critical current of the Bi-2223 tape for cases A to D are 11.19, 11.90, 12.57 and 13.57 A, respectively, whilst the corresponding forces are 555, 641, 545 and 445 N. If the maximum force is required, location B is definitely the best choice. However, it is worthwhile noting here that at the location B the working condition B lies

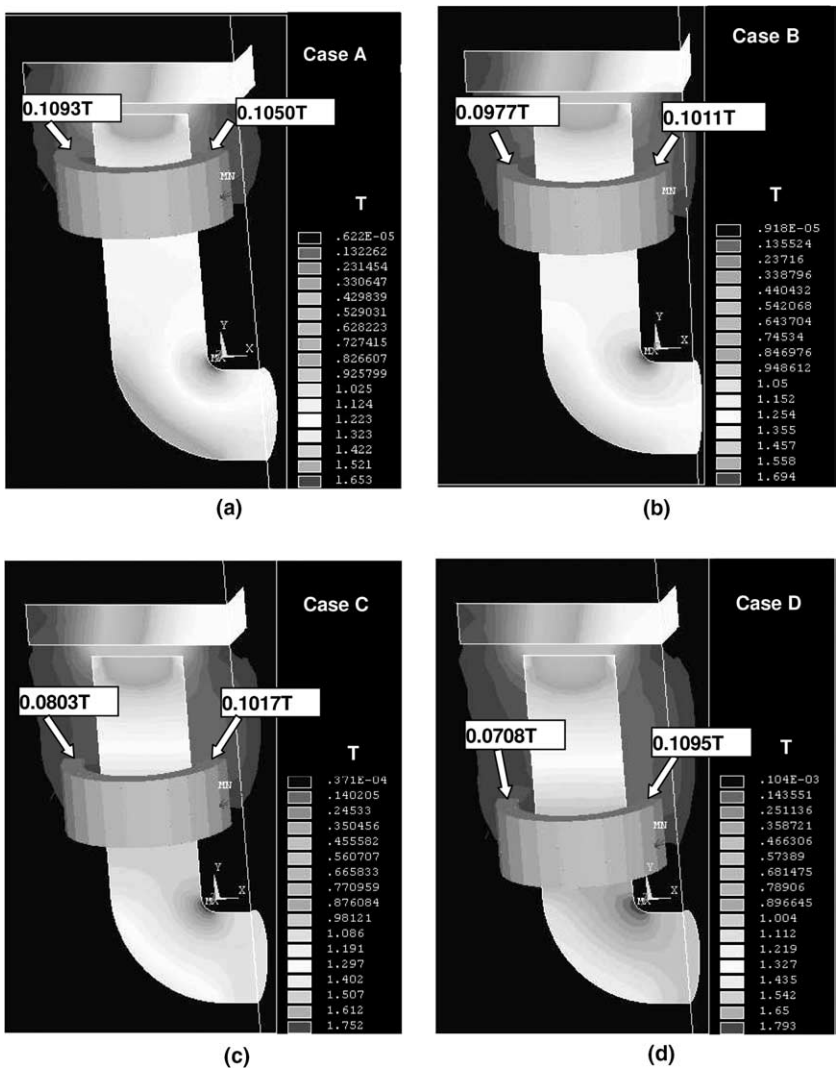

Fig. 10. Flux distribution of the magnetic circuit with coils located at different points. Note that the field marked in R1 and R2 corresponds to the field in the direction parallel to the *X*-axis.

partially in a non-linear force–current region. Operation in this region is not destructive, but would require a fairly complex controller design. Therefore, in most cases location A is commonly chosen. For comparison, the ANSYS-calculated forces for each case are also included in Fig. 9. The maximum error compared with the experimental value is less than 10%. This agreement demonstrates the suitability of this method as a basis for system design. And thus the simulated force–current curve in the situation where the coil was assumed to be located at the back leg of the U-shape iron core is also plotted in Fig. 9. It is clear that although the the radial component field in the coil winding may be greatly reduced by this structure, the early attainment of the saturation point limits the full performance as a whole. Theoretically speaking, for a cylinder shape, the middle part of the iron core is more likely to be magnetized than the part near the pole surface, due to the demagnetization effect. For a general copper based levitation device, the coils are always

located near the pole surface. Only for HTS coils is it necessary to take into account the voltage–current curve, owing to the field dependent critical current of HTS material. It should be mentioned that all results above are only valid for a U-shape iron core and for HTS coils with the given dimensions.

4. Testing results and discussing

Although an optimized operating point was determined as position B, in practice, any locations was chosen to match the weight requirement of 7.2 kg. Thus, the two coils were located at the bottom of the cryostat, i.e. point D. In this demonstrator, the current needed to balance the self-weight of 7.2 kg was experimentally found to be 3.2 A, giving a flux density at the air gap of 0.21 T. This value is within the linear operating range of the magnetic circuit, and still has a linear region of at least 300% for improvement. In terms of the critical current of the Bi-2223/Ag tape (13.57 A) and the current of 9.93 A at which the iron starts to saturate, if the non-linear property of the iron-core taken into account, there is even more room (400%) for load variation. Similarly, if the design is to be accomplished by using only the linear part of the force–current curve, the number of turns in the coils should be further reduced. This modification in conjunction with the field dependency of the critical current of the Bi-2223 tape, as well as the optimization of the U-shape iron core design are important for further study.

5. Conclusion

The design and test results reported in this paper establish a general process for design and construction of an EMS-based HTS maglev vehicle. A detail experimental and numerical analysis of the influence of the coils location on the critical current of the Bi-2223 tape and force–current of the magnetic circuit core was performed. The key features of the vehicle are as follow.

- Eight Bi-2223 coils, with total tape length of 600 m. The vehicle weights 46 kg, which could produce a maximum net attractive force 340 N in a 5 mm air gap.
- An non-eddy current, light-weight and economical cryostat.
- The system uses state-of-the-art HTS tape and has an immediate potential for using the YBCO tape when available.
- The HTS coil was very stable under the controllability mode and a typical lead-leg controller design method is suitable for use with EMS-based HTS maglev vehicle.

Acknowledgments

We thank Innova Superconductor Technology Co. Ltd. for provision of 600 m of HTS tapes. One of authors would like to thank a number of individuals at the Applied Superconductivity Research Center who were responsible for assembly and construction of the system. In particular, thanks to Liu Shuli for coil fabrication and Shi Aijun for mechanical processing. Special thanks are given to Prof. Duxing Chen who provided much guidance in coil short circuit examination. This project was partly supported by Tsinghua University under contract no. JC2002025.

References

[1] S. Kalsi, M. Proise, T. Schultheiss, B. Dawkins, IEEE Trans. Appl. Supercond. 5 (1995) 964.
[2] S. Kalsi, Appl. Supercond. 3 (1995) 163.
[3] R.G. Jenkins, H. Jones, R.M. Goodall, IEEE Trans. Magn. 32 (1996) 2683.
[4] H. Jones, R.G. Jenkins, R.M. Goodall, C. Macleod, A.A. Abbar, A.M. Campbell, NASA Conference Publication 3336 (1996) 535.
[5] H. Jones, P.E. Richens, D.T. Ryan, R.M. Goodall, Physica B 246–247 (1998) 333.
[6] R.M. Goodall et al., IEEE Trans. Appl. Supercond. 5 (1995) 650.
[7] P. Fabbricatore, C. Priano, M.P. Testa, R. Musenich, P. Kovac, A. Matrone, E. Petrillo, M. Ariante, Supercond. Sci. Technol. 11 (1998) 304.
[8] J. Pitel, P. Kovac, Supercond. Sci. Technol. 10 (1997) 7.
[9] K. Tanaka et al., IEEE Trans. Appl. Supercond. 11 (2001) 3002.